Emission-Free Heat Supply of Residential Districts with Solar Thermal Energy and a Heat Pump Storage System

Dimitri Nefodov, Shengqing Xiao, Markus Richter, Thorsten Urbaneck

Chemnitz University of Technology, Professorship Applied Thermodynamics, Chemnitz (Germany)

Abstract

The European Union is aiming at a massive reduction of annual greenhouse gas emissions. Moreover, due to the ongoing and ever worsening energy crisis, costs for consumers are continously rising. Under these conditions, new concepts for heat supply are once again gaining in importance. One approach to avoiding emissions involves the use of highly efficient collector fields in combination with a heat pump-storage system. Here, supply security and economic efficiency are crucial aspects. This paper deals with the conception and possible implementation variants of a corresponding heat supply centre in a residential area (quarter). TRNSYS (TRNSYS, 2019) was used to simulate the system. Parameter studies show the influence of different variables such as collector area, storage volume, etc. The hydraulic circuit as well as the refrigerant of heat pumps exert high influence on the energy efficiency, the heat production costs and the technical safety of the heat supply centre. A variation of heat pump circuits is presented and discussed. The steady-state simulations were performed with the software EBSILON®Professional (Steag, 2019).

Keywords: heat supply, small-scale district heating, store, heat pump, quarter, dimensioning, solar thermal energy, heat production costs

1. Introduction

The European Union aims at reducing annual greenhouse gas emissions by 55% by 2030. It is envisaged that by 2050 Europe should be climate neutral (BPA, 2020). For several months now, the prices of fossil fuels have been rising very sharply leading to a comprehensive increase of costs in all areas of life, i.e., it is a significant macroeconomic phenomenon. In order to counteract these developments and trends in the long term, it is necessary to implement concepts which are largely independent of economic and political developments. Solar thermal energy, photo voltaics (PV) and wind energy are suitable as basic renewable energy sources, which is known for many years. The implementation plans so far, especially in heat supply, have never been failed due to the technical, economic or ecological potentials. Singular considerations (e.g., comparison of the heat production costs without consideration of subsequent costs) often prevents the necessary entry and expansion of solar technologies.

Within the scope of the project „Demonstration of German Energy Transition in Zwickau“ (Leonhardt et al., 2018; Projektträger Jülich, 2019), concepts (such as decentralised and centralised heat supply centres, using digital technologies to minimise the heating load, mobility solutions, etc.) of a comprehensive transformation for the Marienthal residential district (quarter) in Zwickau into a zero-emissions district (living lab) were developed from 2017 to 2022. This paper deals only with the central heat supply. To avoid emissions, the heat supply system must use very high shares of renewable energy (e.g., wind power, PV, solar thermal energy). Other objectives of this subproject are the security of supply and low-heat production costs. The last point particularly takes into account the social aspect of an affordable heat supply. Relatively low and stable prices are especially important considering acceptance by residents. In order to fulfil the above-mentioned objectives, an optimal design is necessary. Against this background, the EBSILON®Professional (Steag, 2019) and TRNSYS 18 (TRNSYS, 2019) software packages were used for optimisation purposes. The presented investigations are divided into two parts. In the first part TRNSYS was used for modelling and simulation of the heat supply system. This simulation also allowed parameter variations (see section 4). The key performance indicators are then used to assess the fulfilment of the objectives. The system under study uses compression heat pumps with fixed coefficient of performance $\varepsilon_{\mathrm{HP}}$. When using solar thermal energy as a heat source, several challenges may arise for the heat pumps. For example, a large temperature range between the heat source and the heat sink as well as variable source temperatures from the solar thermal system are determinants of the

Selection and/or peer review under responsibility of Scientific Committee
doi:10.18086/eurosun.2022.08.08 Available at http://proceedings.ises.org

system operation and the coefficient of performance. In the second part based on modelling and simulations using EBSILON, the influence of the design of the heat pump circuit and the used refrigerant were investigated.

In comparison to the preliminary works (Hornberger, 1994; Raab, 2006; Marx, 2015) (solar local heating systems with heat pumps: The combination of solar thermal systems together with heat pumps has been applied for a long time. A detailed description is provided by (Nefodov, 2019).), the system under study has a solar fraction of 100%. In addition, the boundary conditions in the district (e.g., available areas) and unfavourable operating conditions (e.g., stagnation in the collectors) must be considered to ensure the security of supply.

2. Reference district and heat supply system

The reference district of the current considerations is the Marienthal residential district, which is located in the west of the city of Zwickau in Germany. The buildings in this district are three- or four-storey GDR (*German Democratic Republic*) -type buildings, which were built between 1957 and 1964 (Leonhardt et al., 2018). They were renovated after 1990 and insulated according to the regulations at that time. Natural gas fired boilers cover the space heating (supply and return temperatures of 70 and 55 °C), and domestic hot water heating is partly provided by electric instantaneous water heaters. For both, change was sought. Further modernisation of the existing buildings was not planned. Marienthal district offers excellent conditions for a local heating supply and already has a local heating network which needs to be modernised.

In Fig. 1, the electrical-thermal interconnection system is shown including the balance limits (several technical solutions were investigated in the project, which are not presented here). The main point of the present work relates to the local heating system (central heat supply). The balance limit of interest here is described using the term “heat supply” in Fig. 1. I.e., the supply of electrical energy and the purchase of renewable electricity are initially hidden. The technical approach provides the following essential points:

- use of highly efficient collectors to form a large-scale and cost-effective field,
- use of compression heat pumps,
- use of water stores (5…95 °C) with low losses and very good stratification behaviour (Urbaneck, 2018a, 2018b),
- optional securing of the local power supply with an electrochemical storage system. As part of another subproject, the heat recovery was planned here.

The operating mode for the local heating system is described below. In the case of high irradiation in summer, both storage tanks TES1 and TES2 can be loaded directly via the collectors. Storage tanks operate as seasonal thermal energy storages at a high-temperature level to exploit the solar irradiation potential during the summer. Discharge in summer and autumn takes place directly, which makes the heat pumps unnecessary. In the winter period, the heat pumps use heat water store TES1 as a heat source and charge heat water store TES2 at high temperatures. During the winter and transition periods, the collector field operates at low temperatures, whereby the specific yield increases significantly. At low temperatures in the water store TES1, two-stage operation with HP1 and HP2 is planned for technical and energy reasons. The operation of heat pumps depends on the supply of electricity from renewable energy sources in order to keep CO_2 emissions as low as possible. Thereby the water store TES2 decouples heat load from heat pump operation. The heat pumps and auxiliary units are powered by renewable electricity, which can be obtained from the electrical grid or local PV fields. Further information can be found in Leonhardt et al. (2018) and Nefodov et al. (2019).

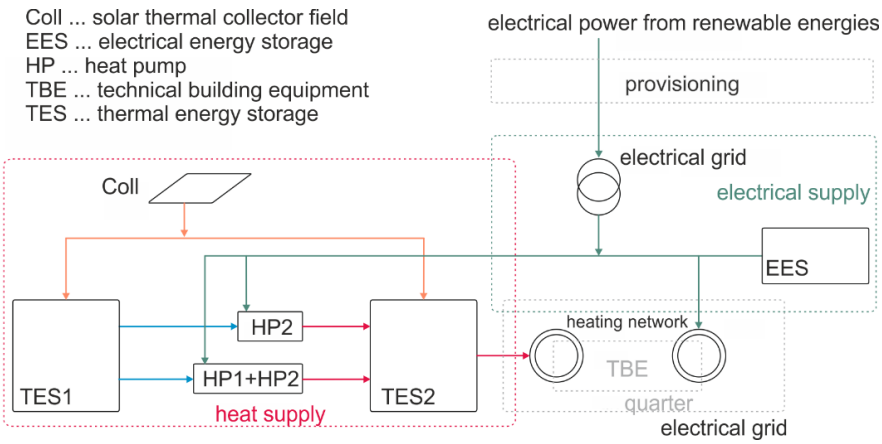

Fig. 1: Electrical-thermal interconnection system with central organisation, scheme of the technical concept and energy flows as well as balance limits (Urbaneck, 2017a)

3. System modelling with TRNSYS

The local heating system (Fig. 2) was modelled and simulated using the simulation software TRNSYS. Meeting the project objectives requires an optimal design and an optimal system operation. For this reason, after modelling, many simulations were carried out with parameter variations (e.g., size of the collector field and storage tank). Subsequent parametric studies show the influence of important parameters (e.g., size of the collector field, heat production costs, etc.), which allows a targeted system design.

In this paper, the heat supply for 133 residential units (7,776.5 m² usable area A_Q. This variant only supplies a relatively small part of the district. Here, from a practical point of view, only solar radiation is available as a heat source) is investigated. The annual heat demand Q_{Net} is approx. 908 MWh a^{-1}, and the test reference year TRY2011 (Zone 9) (DWD, 2018) was chosen as the data basis for the climatic boundary conditions. Technical specifications of a large-area collector were used as parameters for the collector area (TRNSYS type 1: solar collector). The following parameters of the collector efficiency equation were assumed: visual efficiency 85.7 %, linear heat loss coefficient 3.083 W m^{-2} K^{-1}, quadratic heat loss coefficient 0.013 W m^{-2} K^{-2}. The field has a slope of 45 ° and is ideally oriented towards the south. Furthermore, both Thermal Energy Storages (TES1 and TES2, Fig. 1) have been combined into a single heat storage tank (TRNSYS type 340: stratified fluid storage tank) with the height-to-diameter ratio of one. In this case, the heat storage tank has two temperature zones (high-temperature (ht) and low-temperature zone (lt) as illustrated in Fig. 2). The compact storage tank therefore has relatively low heat losses.

In the TRNSYS simulation, no specific heat pump (the selection of suitable refrigerants for heat pumps is described in Xiao et al. (2022)) was modelled. Initially, a simple heat pump model with a constant coefficient of performance of 3.3 was used. This is a simplification, which is necessary in the first step to understand the system behaviour and to make a first dimensioning. This constant value corresponds to the annual performance factor of a typical heat pump (the value was calculated by means of EBSILON simulations, product research confirms this value). The heat pump model consisted of a cooler (TRNSYS type 238, custom-programmed) and a heater (TRNSYS type 138: auxiliary fluid heater), where the cooler represented the evaporator side, and the heater represented the condenser side. This approach made it possible to calculate the heat flows, simplifying the heat pump operation mode. The heat pump model was configured in a way which can cover the maximum network heating load. Moreover, the system had a virtual electric back-up heater to compensate for a lack of heating capacity (e.g., undersizing of the collector array, discharged TES1 storage tank, insufficient heating capacity of the heat pump).

Regarding the loads (heating network in Fig. 2), there were no measured values available for the network or the buildings. As the building density in the area is relatively high, the network losses can be assumed to be low. Experience shows that in a network of this type, the annual heat losses are around 7% of the amount of heat consumption (Urbaneck, 2017a; Shrestha, 2019). To calculate the network load (without considering the network heat losses), the building heating loads were created using the software solar computer (module W38: cooling load and room temperature VDI 2078/6007 for Germany) and the domestic hot water heating loads

(domestic hot water profiles according to VDI 6002, part 1 (VDI, 2014)) were used. The influence of the user remains largely unconsidered in the solar computer simulations. The room temperatures according to EN 12831 supplement 1.

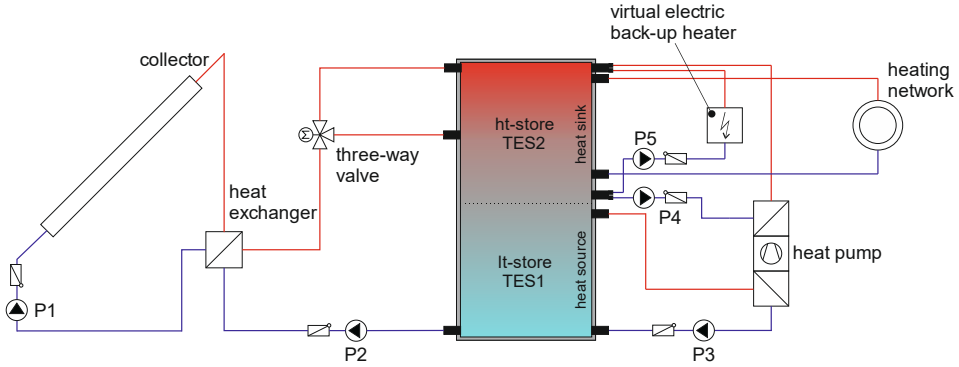

Fig. 2: Scheme of the local heating system and principle structure of the simulation with one heat pump, technical solution for the balance limit heat supply in Fig. 1 (according to Nefodov et al. (2020))

The ordered and normalised values for the network heating load are shown in Fig. 3 a). For a better assessment of the plausibility, three curves are shown in Fig. 3 a):

- the simulated network heating loads (TRY2011 as the basis for the space heating load) without network losses,
- the simulated network heating loads (TRY2011 as the basis for the space heating load) including network losses,
- measured values of the Brühl solar district heating system in Chemnitz (2018) (Urbaneck, 2017a). The heat supply system Brühl is significantly larger than the solution investigated here. However, the network temperatures and the houses (renovated apartment buildings with commercial units) with the corresponding use are partially similar. The climatic conditions also coincide. Therefore the measured values are used for comparison.

In all cases, there is a pronounced peak load range (values from 0.7 to 1.0). In the medium load range (values from 0.2 to 0.7) and in the base load range (values less than 0.2), the simulated values (blue curves) are lower than the measured values of the comparison system. The higher measured values in the medium load range can be explained by the type of use (partly commercial use at the Brühl), the user behavior (e.g., elderly people with high presence time in the apartment) or the occupancy. Load curves calculated for the Marienthal district show that the network losses (as expected) have the highest influence on the base load range.

Monthly heat amount to the network are shown in Fig. 3 b). The conversion of the annual heat demand to the areas in the district provides then the following key figures. The specific annual heat demand (using the simulated values without network losses) is 117 kWh m^{-2} a^{-1} which is related to the net effective area of the building. When converted to the useful building area according to §19 EnEV (BMJ, 2019), the value is then 97 kWh m^{-2} a^{-1}. These values are higher than the data in energy certificates of buildings in the Marienthal district (average of approx. 70 kWh m^{-2} a^{-1} in 2017, useful building area according to §19 EnEV (BMJ, 2019)). Therefore, the uncertainties mentioned above must be considered as well.

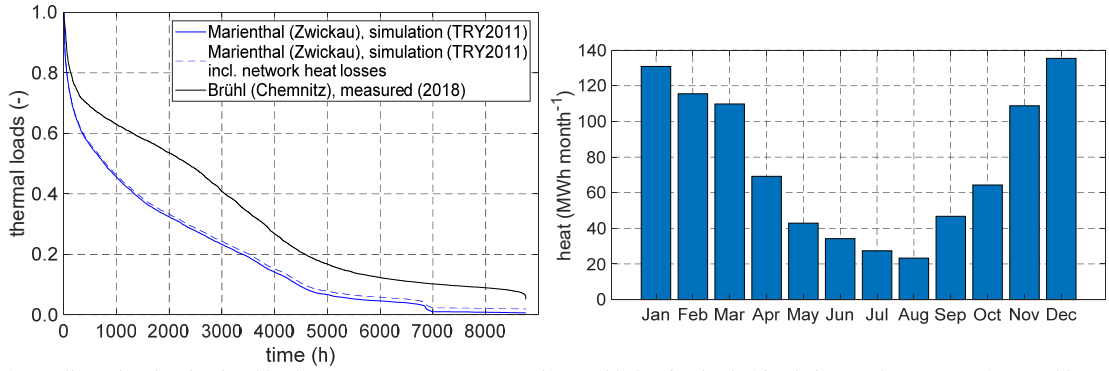

a) non-dimensional and ordered load curves

b) monthly heating loads (simulation results, TRY2011), annual heat quantities of 908.48 MWh a^{-1}

Fig. 3: Standardized network heating loads as well as monthly heat quantities into the heating network (according to Nefodov et al. (2020))

4. TRNSYS parameter study

The two most important parameters of the system are the collector area A_{coll} and the storage volume V_{TES} or storage capacity. In this parameter study these parameters were varied. Thereby, an automatic dimensioning of the system took place (e.g., volume flow in the collector circuit). Otherwise, typical values were used (e.g., thermal insulation of the storage tank). The system's main heating load remained identical in all simulations (Fig. 3:).

The use of non-renewable primary energy is to be minimised. The solar fraction f_{sol} (eq. 1) was used here as the evaluation parameter. In the simulation, the use of virtual back-up heater (Fig. 2) indicated an under-coverage by the collector array or heat pump. I.e., only at this point was non-renewable primary energy used. In case of a total avoidance of non-renewable primary energy, the solar fraction assumes 100%. The losses, which occur in particular with seasonal storage was also considered by eq. 1. Furthermore, the electricity provided for the heat pump must come from renewable energy sources (e.g., photovoltaic system, wind power). If the parameter f_{sol} takes a value of 100%, it means that the heat supply is emission-free. Otherwise, it is fraught with emissions.

$$f_{\mathrm{sol}} = \left(1 - \frac{Q_{\mathrm{VH}}}{Q_{\mathrm{Net}} + Q_{\mathrm{TES,loss}}}\right) \cdot 100 \qquad \text{(eq. 1)}$$

The dependence of the solar fraction on the collector area and the storage volume is shown in Fig. 4. Relatively large collector areas and storage volumes are necessary to completely cover the given heat load. The shown area of the solar fraction has a relatively even course. Theoretically, several system variants achieve a solar fraction f_{sol} of 100% (equivalent for an emission-free heat supply). Further analyses are to find an optimal design.

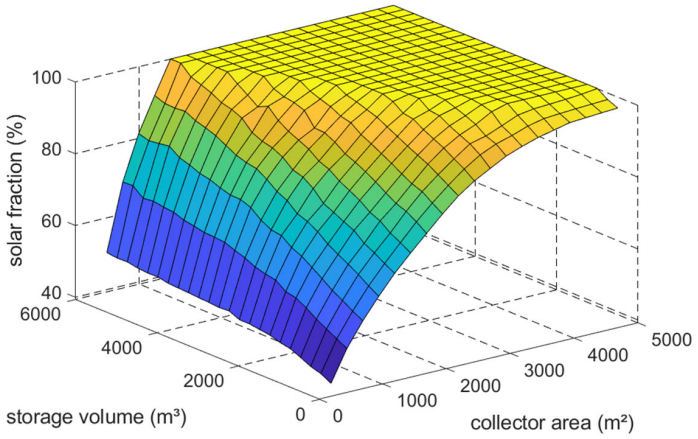

Fig. 4: Influence of the collector area and storage volume on the solar fraction, TRNSYS simulations (according to Nefodov et al. (2020))

Low heat production costs are the next evaluation parameter in this investigation. After the automatic dimensioning of the components, the investment costs were calculated on the basis of specific costs (values, functions, the reference year for the economic calculations is 2019). These investment costs were then included in the calculation of the heat production costs based on the VDI 2067. The annuity factor in the present case was 6.51% (5% interest, 30 years technical service life for all components). The heat pump operation requires a very high amount of electricity, so this cost group has a major influence. The electricity costs here were 0.16 € kWh^{-1}. Furthermore, planning, land, development and investment costs for virtual back-up heater as well as value added tax and a financial subsidy were not considered.

The heat production costs k_{h} are shown in Fig. 5 a). For better orientation, the following diagrams show the isolines (black dash lines) for the solar fraction f_{sol} of 50%, 80% and 100%. It should also be noted that in systems with high solar fractions or with an increasing ratio of collector area to storage volume, stagnation cases occur more frequently. These stagnation cases lead to a failure of the collector circuit for at least one day, to an increased thermal load on the system and possibly to consequential damage as well as to additional operation-related costs (e.g., personnel deployment for control and recommissioning). For the present evaluation, it was determined that the additional costs are 2,000 € per day with stagnation (according to assumptions, no specific measures are foreseen to avoid stagnation). The usual hourly consideration of the stagnation time does not provide information on how many days per year the system is out of operation. For this reason, it is useful to specify the number of days when stagnation occurs. In the following diagrams (Fig. 5, Fig. 6), two borderlines (red dotted lines) have been drawn for the number of stagnation days (1 and 30 days). These two borderlines divide each diagram into three sections. No stagnation occurs in the left section. I.e., the system operation proves to be safe. In the transition zone, between both limits for the stagnation time of 1 and 30 days, stagnation cases occur with increasing frequency. In the last section, the frequency of failures increases to such an extent that it is generally not advisable to design in this area for safety reasons.

In order to achieve the objective, a solar fraction of 100% is appropriate. Under consideration of the above mentioned aspects and additional costs, the optimal heat production costs in Fig. 5 a) (points L_{C1}, L_{C2}, cf. with Tab. 1) on the boundary curve for f_{sol} of 100% lie in the left-hand diagram area. I.e., optimal conditions are at low ratios of collector area to storage volume.

Fig. 5 b) additionally shows the specific investment costs $k_{\mathrm{I,spec}}$ for the systems. The investment costs here are set in relation to the annual network heat load. Increasing values indicate specifically high investments. Fig. 5 b) shows that for the f_{sol} limit curve of 100% the values are in a certain cost range. When the above-mentioned aspects are disregarded, design points in the right-hand diagram area would also be possible.

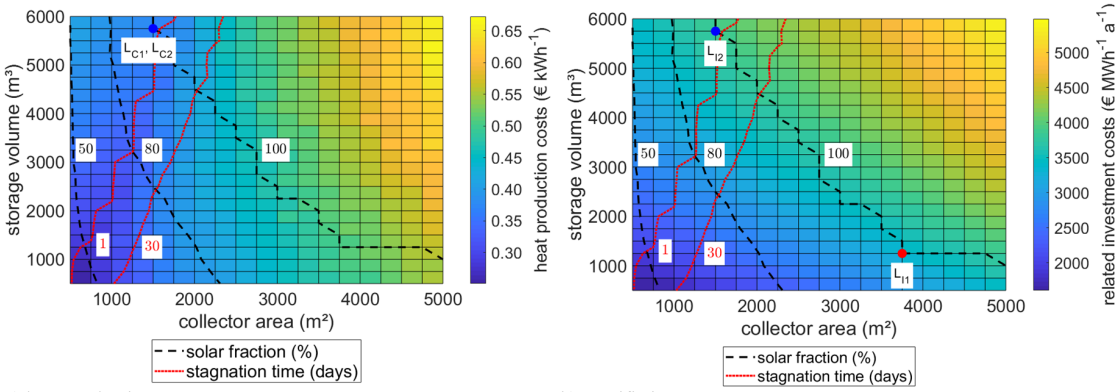

a) heat production costs b) specific investment costs

Fig. 5: Costs for different system dimensions (according to Nefodov et al. (2020))

The system requires floor area, in particular for the collector field, the storage tank and for a building (technical centre). The simplified view neglects, e.g., pipeline routes. Here it is assumed that the collector field is realised as a free-standing installation (a theoretically closed surface). This means that a minimal amount of land is used for the field. Other field constructions (e.g., roof integration on the respective buildings) and system concepts (e.g., three- and four-pipe systems) remain unconsidered. In this consideration, the urban development aspect of the consumption of floor area A_{F} for the system according to Fig. 2 should also be taken into account. The district is relatively densely built up. Distances between the existing buildings and new buildings

(e.g. supply centre) should be maintained. Existing green spaces (e.g., with laundry place or playgrounds) must be preserved at all costs. On the periphery of the district, many areas (e.g., gardens, garages) are not available for the installation of technical equipment. This is why variants with minimal land use are interesting here and in other cases as well.

Fig. 6 provides an estimate of the minimum required floor areas A_F for the system. The point $L_{a,min}$ marks the point with a minimum ground area (1,686 m²). At the same time, the secondary conditions apply that the solar fraction is 100% and no stagnation occurs. The optimum design is again in the left diagram area with low collector area-storage volume ratios.

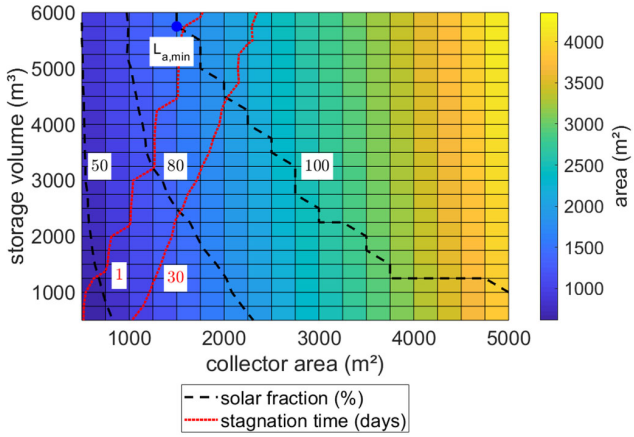

Fig. 6: Estimation of the minimum area required for the system, idealised assumptions (according to Nefodov et al. (2020))

Tab. 1 provides an overview of the discussed points L. Index 1 shows the minimum costs in each case. With index 2, the previous variants are additionally evaluated according to the minimum floor area requirement. Tab. 1 also shows key figures that are suitable for a system comparison.

Tab. 1: Overview of the points with an design according to the given criteria and key figures (according to Nefodov et al. (2020))

Location	A_{coll}	V_{TES}	A_F	k_h	$k_{I,spec}$	$\frac{A_{coll}}{V_{TES}}$	$\frac{A_{coll}}{Q_{Net}}$	$\frac{A_{coll}}{A_Q}$
	(m²)	(m³)	(m²)	(€ kWh^{-1})	(€ MWh^{-1} a^{-1})	(m² m^{-3})	(m² MWh^{-1} a^{-1})	(m² m^{-2})
L_{c1})	1,500	5,750	195.0	0.37		0.261	1.65	0.193
L_{c2})	1,500	5,750	195.0	0.37		0.261	1.65	0.193
L_{I1})	3,750	1,250	310.5		3,447.06	3.000	4.13	0.482
L_{I2})	1,500	5,750	195.0		3,924.44	0.261	1.65	0.193

By considering the stagnation cases in the cost calculations (Fig. 5 a)), there is an overlap of the points L_{c1} and L_{c2}. Thus, the minimum heat production costs are the same in both cases. The minimum specific investment costs (Fig. 5 b), point L_{I1}) are in an unfavourable range with a very high number of stagnation cases. By additionally considering the floor area requirement (Fig. 6), it turned out that the costs for L_{I2} also become minimal in the L_{c2} point. The key figures in Tab. 1 show relatively small collector areas. This seems plausible because seasonal storage is required. These ratios are approximately consistent with the literature sources or similar works (Hornberger, 1994), (Marx, 2015), (Raab, 2006).

The point L_{c2}) therefore provides the values for an optimal design of the system. With a more exact modeling of the system(e.g. heat pump operation, purchase of renewable electricity) or the boundary conditions are changed, a shift in the points shown is possible or probable.

5. Further investigations of heat pump circuits

Xiao et al. (2020) presented detailed research of the six heat pump circuits for use in the ZED project. Initially, the refrigerant R134a was used. This refrigerant damages the ozone layer and should be avoided in future applications. For this reason, further investigations were carried out. The refrigerant R134a was changed to R1234ze(E) (GWP < 1) (Regulation, 2017; Honeywell, 2017) as substitute refrigerant. To make it easier to compare the variants later, an ending was added to the variant number. Refrigerant R134a is used with the

suffix "a" and refrigerant R1234ze(E) with the suffix "ze". Tab. 2 provides an overview of the circuits considered and the attainable coefficients of performance for refrigerant R134a from Xiao et al. (2020). This section compares selected heat pump circuits (variants 1, 5 and 6 according to Xiao et al. (2020)) for both refrigerants, with the aim of identifying the advantages and disadvantages.

Tab. 2: Overview of the investigated heat pump circuits (according to Xiao et al. (2020))

variant	name	ε_{HP} (-)
1a	single-stage compression	2.62
2a	two-stage compression with subcooler economiser	3.02
3a	two-stage compression with an open-flash-economizer	3.13
4a	refrigerant circuit cascade	3.03
5a	series connection a) with common connections to the storage tank	3.21
6a	series connection b) with separate connections to the storage tank	4.16

In the following discussion, the relevant circuits (without consideration of the refrigerants) are presented first. The circuit for the heat pump system with single-stage compression (variant 1, Fig. 7) has a simple structure. Here, the essential components are: an evaporator, a condenser, an expansion valve and a compressor. With this variant, the refrigerant will be compressed directly from the evaporating pressure up to the condensing pressure. The single-stage compression heat pump process behaves less favourably with increasing pressure ratio p_c/p_0 due to the increasing compressor losses and the decreasing volumetric efficiency.

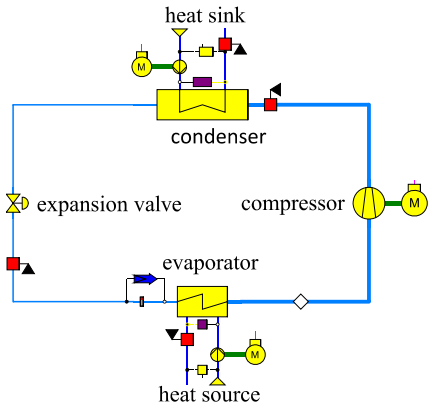

Fig. 7: Heat pump system with single-stage compression (EBSILON model), variant 1 (according to Xiao et al. (2020))

Compared to other variants, variants 5 and 6 proved to be advantageous during the investigations (Xiao et al., 2020). Here, a series connection of two single-stage heat pumps was modelled. In this case, two separate refrigerant circuits exist at different temperature levels.

At variant 5 (Fig. 8), the two refrigerant circuits are coupled with the storage tank through common connections. On the heat sink side, the water from the storage tank flows through two condensers connected in series (inlet temperature 55 °C). On the heat source side, the water is then passed analogue through two evaporators and cooled down (inlet temperature 20 °C). With variant 5, a relatively high temperature spread from 20 K can be achieved on the load side (connection of the heating network). However, with this series connection, the inlet temperature of the storage water on the heat source side (lt-store, Fig. 2) must be above the evaporation temperature in the ht-cycle (Fig. 8). Furthermore, it must be noted that if the temperature on the heat source side (lt-store, Fig. 2) is too low, operation of the ht-cycle (Fig. 8) is not possible. This reduces the available storage capacity on the heat source side.

At variant 6 (Fig. 9), both heat pump circuits have their own connections (heat sink and heat source) to the storage tank and are decoupled. For this reason, the problem mentioned in variant 5 is avoided. Since several charging and discharging devices are required here, a higher technical effort is required for storage design and operation. In this case the lt-cycle raise on the heat sink side the temperature by 40 to 45 °C and the ht-cycle by 65 to 75 °C.

Following Xiao et al. (2020), the coefficient of performance ε_{HP} is used for the energetic evaluation of heat pump circuits. Boundary conditions of the modelling and simulation are summarised in Tab. 3 and Tab. 4.

Pressure ratios may vary according to system requirements. The refrigerant mass flow of the lt-cycle of variant 6 is controlled in such a way that the heat output of the lt-cycle covers the heat extraction of the ht-cycle.

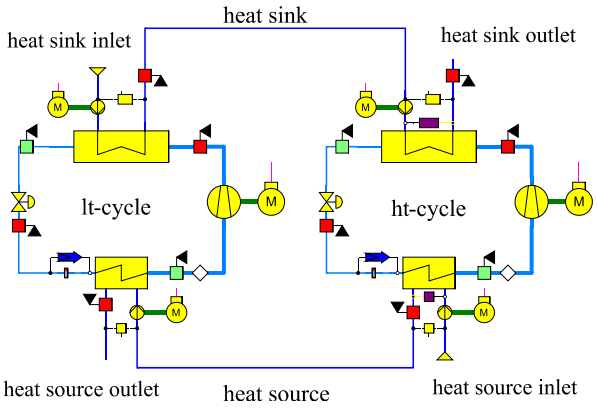

Fig. 8: Heat pump system with series connection a) (EBSILON modell), variant 5 (according to Xiao et al. (2020))

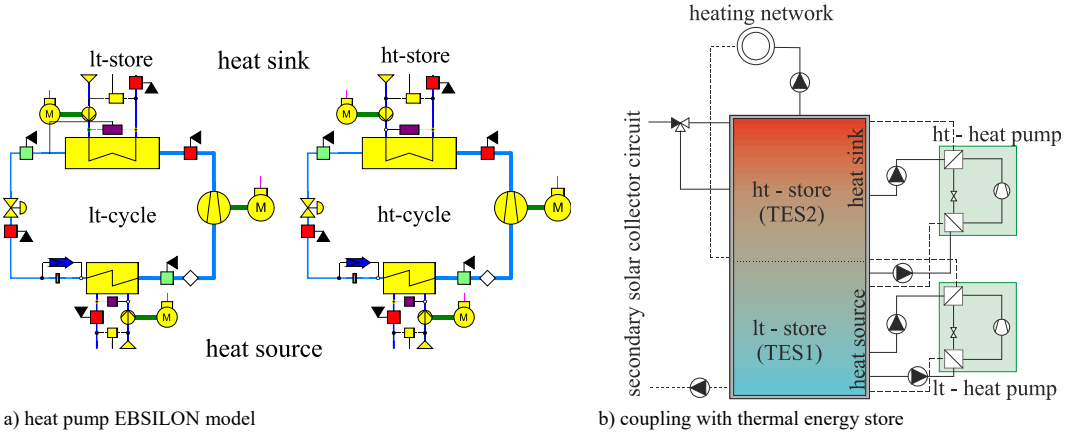

a) heat pump EBSILON model

b) coupling with thermal energy store

Fig. 9: Heat pump system with series connection b), variant 6 (modified according to Xiao et al. (2020))

Both variants 5 and 6 have two circuits. This allows the coefficients of performance of the lt-cycle and ht-cycle to be considered separately. The system coefficients of performance $\varepsilon_{HP,total}$ of both variants are shown in Tab. 5 and Fig. 10. Here, the coefficient of performance $\varepsilon_{HP,total}$ represents ratio of provided heat after each cycle (lt-, ht-cycle) to the electrical effort of the compressors.

The simulation results clearly show the influence of the selected refrigerants. With variant 1ze, the coefficient of performance ε_{WP} increases by 9.54% compared to variant 1a. At the same time, the heat pump heating capacity decreases by 16.2%. In variant 5, the coefficients of performance $\varepsilon_{WP,total}$ for both refrigerants remain almost identical. There is a slight improvement of 1.55% with the new refrigerant. On the other hand, the heat pump heating capacity drops by 14.08% (lt-cycle) and 14.72% (ht-cycle) compared to the circuit with refrigerant R134a. The highest coefficient of performance is achieved by the variant 6ze. The coefficient of performance increases by 36.30% compared to the circuit with the refrigerant R134a. For the lt-cycle, the heating capacity is identical in both cases. The electricity consumption with the refrigerant R1234ze(E) is reduced by 34.50% compared to the reference. At the ht-cycle, the heating capacity drops by 9.0% compared to reference refrigerant R134a. At the same time, the electricity demand decreases, so that a very high coefficient of performance is achieved overall. In total, the circuits with refrigerant R1234ze(E) show better coefficients of performance, but less heating capacity, than circuits with R134a.

Tab. 3: Basic assumptions for all EBSILON models (modified according to Xiao et al. (2020))

refrigerant	R134a	R1234ze(E)
refrigerant mass flow in the main circuit (kg s^{-1})	1.0	
subcooling of the refrigerant in the condenser (K)	0.0	
inlet temperature. heat sink (condenser) (°C)	65	
outlet temperature. heat sink (condenser) (°C)	75	

refrigerant	R134a	R1234ze(E)
overheating of the refrigerant in the evaporator (K)	10	5
inlet temperature. heat source (evaporator) (°C)	15	
outlet temperature. heat source (evaporator) (°C)	10	
pressure drop in heat exchanger (bar)	0…0.05	
minimum value for the pinch point in the heat exchangers (K)	3.0	
isentropic efficiency of the compressors (-)	0.85	
mechanical efficiency of the compressors (-)	0.99	
mechanical loss of the compressors (kW)	0.0	

Tab. 4: Further boundary conditions for the evaluation of the EBSILON circuit models (modified according to Xiao et al. (2020))

	variant 5	variant 6
supply temperature, heat source, lt-cycle (°C)	15	
supply temperature, heat source, ht-cycle (°C)	20	45
supply temperature, heat sink, lt-cycle (°C)	55	40
supply temperature, heat sink, ht-cycle (°C)	65	
refrigerant mass flow, lt-, ht-cycle (kg s^{-1})	1	

Tab. 5: Summary of the simulation results for the circuit models considered (modified according to Xiao et al. (2020))

Variant	Refrigerant	$\dot{Q}_c$ (kW)	$\dot{Q}_0$ (kW)	P_{el} (kW)	ε_{HP} (-)
1a	R134a	145.68	90.09	55.51	2.62
1ze	R1234ze(E)	122.07	79.44	42.51	2.87

Variant	Refrigerant	lt-cycle				ht-cycle				$\varepsilon_{HP,total}$ (-)
		$\dot{Q}_{c,lt}$ (kW)	$\dot{Q}_{0,lt}$ (kW)	$P_{el,lt}$ (kW)	$\varepsilon_{HP,lt}$ (-)	$\dot{Q}_{c,ht}$ (kW)	$\dot{Q}_{0,ht}$ (kW)	$P_{el,ht}$ (kW)	$\varepsilon_{HP,ht}$ (-)	
5a	R134a	155.84	110.03	45.99	3.39	142.82	96.01	46.93	3.04	3.21
5ze	R1234ze(E)	133.89	94.52	39.53	3.39	121.79	83.00	38.86	3.13	3.26
6a	R134a	104.69	75.92	28.29	3.70	133.33	103.92	28.98	4.60	4.16
6ze	R1234ze(E)	104.69	85.53	18.53	5.65	121.34	99.50	21.37	5.68	5.67

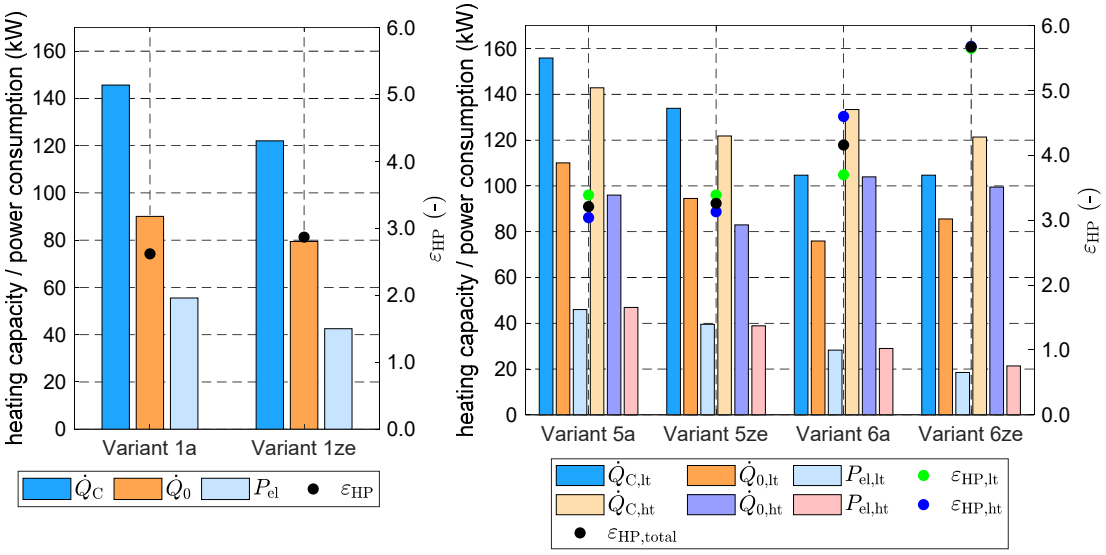

Fig. 10: Summary of the simulation results for circuit models (modified according to Xiao et al. (2020))

6. Summary and outlook

In the present paper, the feasibility and a concept for a solar local heating supply with the use of heat pumps were investigated. A heat supply in the Marienthal district (Zwickau, Germany) is possible with 100% renewable energy. The parameter study has shown that the large number of possibilities are severely limited by technical and economic criteria as well as the amount of floor space required in the district. The investigation provides preliminary parameters and key figures for an optimal system design.

The heat production costs for emission-free supply provide a moderate value of 0.37 € kWh^{-1} (for comparison: Solar local heating systems without heat pumps could achieve solar fractions of f_{sol} = 40…50 % in Germany (no emission-free). The solar heat production costs in the period from 1998 to 2004 were in the range of 0.23 € kWh^{-1}. With an increase in the solar fraction, a very strong rise in solar heating costs was observed. Further optimisation of the presented system allows for significant cost reductions, according to experience). It should be noted that the system with seasonal storage is relatively small (heat supply of 133 residential units). With increasing system size, a cost degression is to be expected. Furthermore, the system supplies a residential district with existing buildings, which are largely equipped with conventional heating technology.

Further investigations on the selected heat pump circuits using EBSILON software showed that R1234ze(E) refrigerant is well suited for heat pump operation. Compared to refrigerant R134a, higher coefficients of performance are achieved, but with lower heating capacity. For the assumed conditions, the series connection of two heat pumps with the separate connections to the storage tank is excellently suited for heat supply (variant 6). According to present investigations, a coefficient of performance of 5.67 can be achieved here.

The presented system offers even more possibilities for optimisation. Increasing the number of residential units or increasing the size of the system can further reduce specific investment costs. The inclusion of other heat sources (e.g., sewage water, geothermal energy, etc.) allows to reduce the collector size and increase the coefficients of performance in winter months. The optimisation of the heat pumps and the storage tank as well as the improvement of the system operation and control strategies will be the focus of further investigations.

Acknowledgments

The realization of the project and the scientific work is supported by the Federal Ministry for Economic Affairs and Climate Action (BMWK) on the basis of a decision by the German Bundestag (funding code 03SBE114C). The authors gratefully acknowledge this support and carry the full responsibility for the content of this paper.

References

Bundesministerium der Justiz und für Verbraucherschutz. *Verordnung über energiesparenden Wärmeschutz und energiesparende Anlagentechnik bei Gebäuden*. [Online] Available from: https://www.gesetze-im-internet.de/enev_2007/__19.html [accessed: 20.07.2019].

Der Deutsche Wetterdienst. *Wetter und Klima - Deutscher Wetterdienst - Der DWD*. [Online] Available from: https://www.dwd.de/DE/derdwd/derdwd_node.html [accessed: 08.01.2018].

Honeywell Belgium N.V., 2017. Solstice® ze Refrigerant (HFO-1234ze).

Hornberger, M., 1994. Solar unterstützte Heizung und Kühlung von Gebäuden. Bd. 47, Diss., Deutscher Kälte- und Klimatechnischer Verein, Stuttgart, Universität.

Leonhardt, S., Höhne, E., Neumann, T., Teich, T., Bodach, M., Hoffmann, M., Kretz, D., Hempel, T., Schwind, M., Franke, S., Urbaneck, T., Gill, B., Schneider, M., 2018. Demonstration einer energieeffizienten und sozialgerechten Quartiersentwicklung auf Basis elektrisch-thermischer Verbundsysteme in Zwickau Marienthal – Projekt ZED: Zwickauer Energiewende demonstrieren, in: Pöschk, J. (Eds.), Energieeffizienz in Gebäuden – Jahrbuch 2018. VME – Verlag und Medienservice Energie, Berlin, pp. 147-154.

Marx, R., 2015. Integration von Wärmepumpen in solare Nahwärmeanlagen mit saisonaler Wärmespeicherung. Diss., Shaker, Stuttgart, Universität, Aachen.

Nefodov, D., Xiao, S., Urbaneck, T., 2019. Emissionsfreie Wärmeversorgung – Stand der Technik und ein neuer Ansatz. Lüftung/Klima, Heizung/Sanitär, Gebäudetechnik (HLH), VDI Fachmedien 70, Nr. 9, pp. 90-97.

Nefodov, D., Xiao, S., Urbaneck, T., 2020. Solarthermie als Schlüssel für eine emissionsfreie Wärmeversorgung auf Quartiersebene. Lüftung/Klima Heizung/Sanitär Gebäudetechnik (HLH), VDI Fachmedien 71, Nr. 9, pp. 38-44.

Oppelt, T., Urbaneck, T., Otto, S., Heinrich, I., Schmidt, A., Göschel, T., Uhlig, U., Frey, H., 2018. Development of a software system for optimal operation of heating networks with central solar plant. *ISES EuroSun 2018 Conference – 12th International Conference on Solar Energy for Buildings and Industry.* Rapperswil, Switzerland.

Projektträger Jülich (PtJ) (2019) Solares Bauen/Energieeffiziente Stadt. [Online] Available from: https://www.ptj.de/solares-bauen-energieeffiziente-stadt [accessed: 10.02.2019].

Raab, S., 2006. Simulation, Wirtschaftlichkeit und Auslegung solar unterstützter Nahwärmesysteme mit Heißwasser-Wärmespeicher, Diss., Cuvillier Verlag, Stuttgart, Universität.

Regulation (EU) No 517/2014 of the European parliament and of the Council of 16 April 2014 on fluorinated greenhouse gases and repealing Regulation (EC) No 842/2006. Official Journal of the European Union. 20.5.2014.

Shrestha, N. L., 2019. Internal information. Technische Universität Chemnitz, Chemnitz.

STEAG Energy Services GmbH, 2019. EBSILON®Professional.

The Press and Information Office of the Federal Government (BPA) (2020) *The EU should be climate-neutral by 2050*. [Online] Available from: https://www.bundesregierung.de/breg-en/issues/climate-action/more-climate-protection-in-eu-1797114 [accessed: 21.07.2022].

TRNSYS: A TRaNsient SYstems Simulation Program - Version 18, 2019. Solar Energy Laboratory, Univercity of Wisconsin-Madison und Transsolar Energietechnik GmbH, Stuttgart.

Urbaneck, T., 2017a. Internal information. Technische Universität Chemnitz, Chemnitz.

Urbaneck, T., Findeisen, F., Mücke, J. M., Lang S., Gensbaur, M., Bestenlehner, D., Drück, H., Beyer, R., Pieper, K., 2014 - 2018. Oberirdische Speicher in Segmentbauweise für Wärmeversorgungssysteme – OBSERW; Abschlussbericht zum Verbundvorhaben. 2018a. Förderkennzeichen: 03ET1230A/B/C. [Online] Available from: http://nbn-resolving.de/urn:nbn:de:bsz:ch1-qucosa2-210713 [accessed: 12.02.2019]

Urbaneck, T., Oppelt, T., Sehwöster, I., Bank, E. F., 2018b. Große Druckbehälter als thermische Energiespeicher, Teil 1: Vor- und Nachteile sowie Einsatzgrenzen. EuroHeat&Power, VWEW Energieverlag 47, issue 11-12, pp. 18-23.

Urbaneck, T., Oppelt, T., Shrestha, N. Lal, Platzer, B., Göschel T., Uhlig, U., Frey, H., 2017b. Technische Umsetzung der solaren Fernwärme Brühl. EuroHeat&Power, VWEW Energieverlag 46, issue 11, pp. 20-23.

VDI 6002 Blatt 1, März 2014. Solare Trinkwassererwärmung Allgemeine Grundlagen, Systemtechnik und Anwendung im Wohnungsbau. Beuth Verlag GmbH, Berlin.

Xiao, S., Nefodov, D., McLinden, Mark O., Richter, M., Urbaneck, T., 2022. Working fluid selection for heat pumps in solar district heating systems. Solar Energy, Elsevier 236, pp. 499-511. https://doi.org/10.1016/j.solener.2022.02.036

Xiao, S., Nefodov, D., Urbaneck, T., 2020. Untersuchungen von Wärmepumpenschaltungen – Simulationen von Kompressionswärmepumpen mit großem Temperaturhub und variablen Quelltemperaturen, in: Deutscher Kälte- und Klimatechnischer Verein e. V. DKV (Eds.), Deutsche Kälte- und Klimatagung 2019 Ulm.

Nomenclature

Symbol	Description	Unit
Latin letters		
A	area	m²
f_{sol}	solar fraction	%
k_{h}	heat production costs	€ kWh^{-1}
$k_{\mathrm{I,spec}}$	specific costs	€ MWh^{-1} a^{-1}
P_{el}	electric power	W
p_0	evaporator pressure	Pa
p_{c}	condenser pressure	Pa
Q	heat quantity	MWh a^{-1}
$\dot{Q}_0$	thermal capacity, evaporator	W
$\dot{Q}_{\mathrm{c}}$	thermal capacity, condenser	W
V	volume	m³
Greek letters		
$\varepsilon_{\mathrm{HP}}$	coefficient of performance	-

Indices and abbreviations	
a	area
BMBF	Bundesministerium für Bildung und Forschung (engl.: Federal Ministry of Education and Research)
BMWK	Bundesministerium für Wirtschaft und Klimaschutz (engl.: Federal Ministry for Economic Affairs and Climate Action)
c	heat production costs
coll	Collector
DWD	German Meteorological Service
F	floor
HP	heat pump
ht	high temperature
I	investment costs related to the annual heat load
L	location
lt	low temperature
Net	local heating network
P	pump
Q	living space
TES	thermal energy storage
VH	virtual back-up heater
ZED	Demonstration of German Energy Transition in Zwickau